



The synthesis and structure–activity relationship of substituted *N*-phenyl anthranilic acid analogs as amyloid aggregation inhibitors

Lloyd J. Simons^a, Bradley W. Caprathe^a, Michael Callahan^a, James M. Graham^a, Takenori Kimura^b, Yingjie Lai^a, Harry LeVine III^a, William Lipinski^a, Annette T. Sakkab^a, Yoshikazu Tasaki^b, Lary C. Walker^a, Tomoyuki Yasunaga^b, Yuyang Ye^a, Nian Zhuang^a, Corinne E. Augelli-Szafran^{a,*}

^a Pfizer Global Research and Development, Ann Arbor Laboratories, 2800 Plymouth Rd., Ann Arbor, MI 48105, USA

^b Yamanouchi Pharmaceutical Co., Ltd., Tsukuba Research Center, 21 Miyukigaoka, Tsukuba, Ibaraki 305, Japan

ARTICLE INFO

Article history:

Received 14 October 2008

Revised 10 December 2008

Accepted 11 December 2008

Available online 24 December 2008

Keywords:

Beta-amyloid

Alzheimer's disease

N-Phenyl anthranilic acid

Analogs

Amyloid plaques

Amyloid aggregation

Tg2576 mice

Hsiao mouse model

Amyloid aggregation inhibitors

ABSTRACT

It is believed that β -amyloid aggregation is an important event in the development of Alzheimer's disease. In the course of our studies to identify β -amyloid aggregation inhibitors, a series of *N*-phenyl anthranilic acid analogs were synthesized and studied for β -amyloid inhibition activity. The synthesis, structure–activity relationship, and in vivo activity of these analogs are discussed.

© 2008 Elsevier Ltd. All rights reserved.

Genetic, pathological and biochemical evidence implicates aggregation of β -amyloid ($A\beta$) peptide in the pathogenesis of Alzheimer's disease.¹ Current marketed therapies for Alzheimer's disease are palliative and only modestly effective. A disease-modifying drug would be a major therapeutic breakthrough towards the treatment of this disease.

Our initial attempts at generating small molecule inhibitors for β -amyloid aggregation were based on Congo Red, a well-known stain for amyloid protein fibrils.² Figure 1 depicts the refinement of the structural class from a diazo-linked anthranilic acid derivative to an ethyl-linked moiety. The addition of a single methylene unit in the linker generated compounds with increased in vitro potency. Based on the promising in vitro and in vivo results³ of initial leads PD 0118057 (**14**) and PD 0202091 (**57**), additional synthesis was pursued to generate a structure–activity relationship within this series of compounds.

* Corresponding author at present address: Laboratory for Experimental Alzheimer Drugs (LEAD), Harvard Medical School and Brigham & Women's Hospital, 77 Avenue Louis Pasteur, HIM 756, Boston, MA 02115, USA. Tel.: +1 617 525 5230; fax: +1 617 525 5252.

E-mail address: caugelli@rics.bwh.harvard.edu (C.E. Augelli-Szafran).

In Scheme 1, olefin **3** was generated from heating a pyridine solution of *p*-nitrophenylacetic acid **1** and substituted aldehyde **2**. Hydrogenation of **3** gave amine **4** which was then coupled with

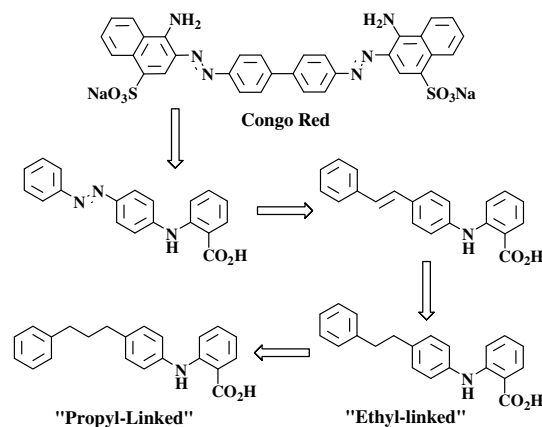
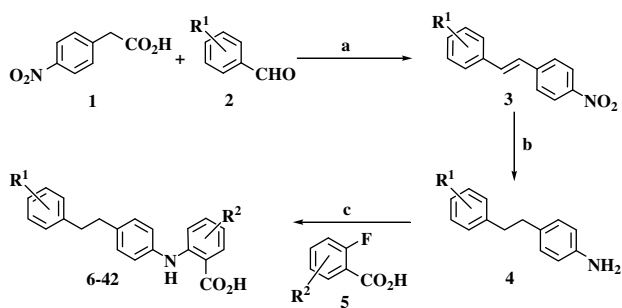
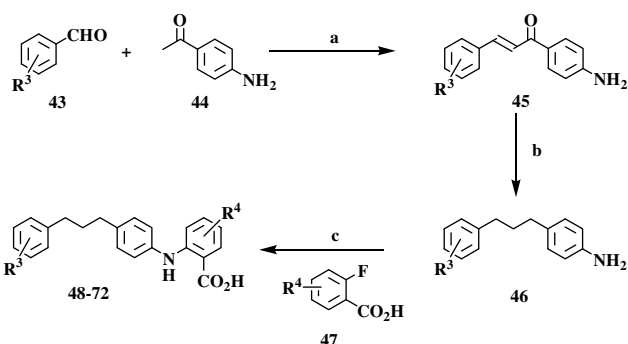


Figure 1. Evolution of *N*-phenyl anthranilic acid analogs as amyloid aggregation inhibitors.



Scheme 1. Reagents: (a) Pyr; (b) RaNi, H₂, THF; (c) LHMDS, THF.



Scheme 2. Reagents: (a) NaOH, EtOH or H₂SO₄, AcOH; (b) Et₃SiH, TFA; (c) LiNH₂, THF.

Table 1
Modifications of ethyl-linked derivatives

Compound	R ¹	BASSR IC ₅₀ (μM)	BASST IC ₅₀ (μM)
6	4-OMe	>100	>100
7	<i>N</i> -DHIQ ^a	>100	1
8	H	60	10
9	3,4-Me	>100	10
10	2-Cl	>100	5
11	3-Cl	>100	19
12	4-Cl	>100	3
13	3-F	>100	70
14	3,4-Cl	>100	2
15	2,4-Cl	>100	51
16	3,5-Cl	>100	15
17	3,4-F	>100	2
18	4-F, 3-CF ₃	>100	2
19	3-Cl, 4-Me	88	1

^a *N*-decahydroisoquinoline.

2-fluoro benzoic acid **5** in the presence of a strong base to give ethyl-linked derivatives **6–42**.

Propyl-linked derivatives (Scheme 2) were prepared via an acid-base-catalyzed Aldol reaction. Reaction of substituted aldehydes **43** and 4-aminoacetophenone **44** generated chalcone **45**. Reduction of chalcone **45** gave propyl-linked anilines **46** that were subsequently coupled with 2-fluoro benzoic acids **47** to yield the corresponding propyl-linked anthranilic acids **48–72**.

The *in vitro* data were obtained from two primary assays, BASSR and BASST, which were designed to determine the inhibition of amyloid fibril formation by the test compound. BASSR (Beta-Amyloid-Self-Seeding Radioassay) is a radiolabeled ¹²⁵I-Aβ(1–40) filtration assay. The BASST (Beta-Amyloid-Self-Seeding, Thioflavin T) is an amyloid-specific fluorescence assay. The test compound was incubated under the same conditions in both assays with Aβ(1–40)/buffer (30 μM unlabeled Aβ(1–40)/50 mM NaPi–150 mM NaCl, 1 M urea, 0.02% w/v NaN₃, pH 7.5). In the BASSR assay, a tracer amount of ¹²⁵I-labeled Aβ(1–40) was added to the assay. In the BASST assay, 5 μM ThioflavinT (ThT) was added after fibril formation.⁴ BASST reports on the formation of the β-sheet structure of amyloid fibrils.⁵ This measure can be complicated by false positives that result from the competition of test compounds with the extrinsic fluorescent ThT probe for binding to amyloid fibrils. Therefore, an additional assay, BASSR, was used to detect the inhibition of peptide aggregation. BASSR measures the formation of the radiolabeled fibrils that do not pass through a 0.2 μm filter. These two assays provided complementary information about the aggregation state and fibrillar amyloid conformation with compound present. Eight concentrations of each compound were used for IC₅₀ determinations that were calculated by logit transformation of the titration curves. Variation of individual points was ±10%. The average IC₅₀s of two separate experiments are reported. At 30 μM of Aβ(1–40) peptide, an inhibitor with an IC₅₀ of 1 μM targets a species that is less than 3% of the total peptide concentration. These assays were designed to detect inhibitors at an early stage in fibril formation with an amount of compound that would be less than the Aβ(1–40) peptide monomer concentration. An IC₅₀ of 20 μM is approximately equivalent to a ratio of 0.7 moles compound/peptide monomer and thus, is borderline substoichiometric.^{4,5} (The observed IC₅₀ is a product of the true affinity of the compound, the stoichiometry of binding, and the concentration of the target aggregation intermediate.)

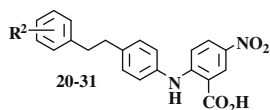
In vivo efficacy studies were performed in Tg2576 mice that over-express human βAPP695_{Swe}. These mice show an age-related increase in cerebral Aβ deposition, and therefore, are suitable models for testing β-amyloid aggregation inhibitors.⁶ Bioavailable and brain-penetrant compounds were delivered orally by mixture in chow.

Our initial efforts in the ethyl-linked series produced a series of compounds (Table 1) that showed acceptable activity in the BASST assay, but were inactive in the BASSR assay.

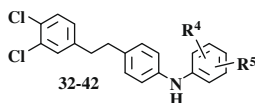
By adding a nitro group to the anthranilic acid ring (Table 2), potency increased significantly in both assays. However, the nitro functionality is considered to be a risk for CNS compounds since it may decrease brain-penetration of the compound or have potential toxicity. Therefore, other substituents on the anthranilic acid ring were explored (Table 3).

When the carboxylic acid group was moved to the 4- and 5-positions on the aromatic ring (entries **32** and **34**, Table 3 vs entry **14**, Table 1), a 5-fold decrease in potency in BASST was observed. The methyl ester analog (entry **33**) of entry **32** exhibited no activity in either BASST or BASSR. Some of the most potent derivatives of **14** had a carboxylic acid group in the 6-position and an electron-deficient anthranilic acid ring (see Table 2 and entries **37**, **39** and **41** in Table 3).

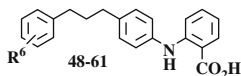
By increasing the length of the alkyl linker by one methylene unit (i.e., propyl-linked, Table 4), a significant increase in potency was observed in the BASSR assay relative to the similarly substituted inactive ethyl-linked compounds (entries **50**, **52**, **54–56** in Table 4 vs **8–12** in Table 1). In addition to this observed increase in potency, another advantage of the propyl-linked analogs was the consistent activity in both BASSR and BASST. However, substitution on the anthranilic ring of the propyl-linked analogs with electron withdrawing groups (Table 5, entries **65**, **66**) did not give

Table 2
4-Nitro substitution of ethyl-linked derivatives

Compound	R ²	BASSR IC ₅₀ (μM)	BASST IC ₅₀ (μM)
20	4-N(<i>n</i> Bu) ₂	15	1
21	DHIQ ^b	5	1
22	H	70	1.5
23	3,4-Me	12	2
24	2-Cl	3	0.5
25	3-Cl	33	0.3
26	4-Cl	15	0.4
27	3,4-Cl	43	0.5
28	2,4-Cl	17	4
29	3,4-F	41	4
30	4-F, 3-CF ₃	3	0.8
31	4-Cl, 3-CF ₃	16	1

^b N-decahydroisoquinoline.**Table 3**
Other modifications of ethyl-linked derivatives

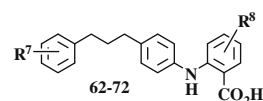
Compound	R ⁴	R ⁵	BASSR IC ₅₀ (μM)	BASST IC ₅₀ (μM)
32	H	4-CO ₂ H	>100	10
33	H	4-CO ₂ Me	>100	>100
34	H	5-CO ₂ H	>100	10
35	4-CF ₃	5-CO ₂ H	>100	35
36	4-F	5-CO ₂ H	>100	3
37	2-aza ^c	6-CO ₂ H	7	2
38	4-Me	6-CO ₂ H	>100	2
39	3-CF ₃	6-CO ₂ H	27	4
40	2-CF ₃	6-CO ₂ H	>100	30
41	5-CF ₃	6-CO ₂ H	70	0.1
42	4-NEt ₂	6-CO ₂ H	>100	53

^c substituted pyridine ring.**Table 4**
Propyl-linked derivatives

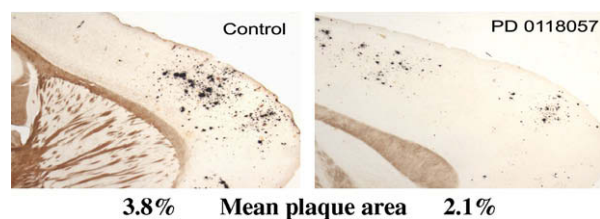
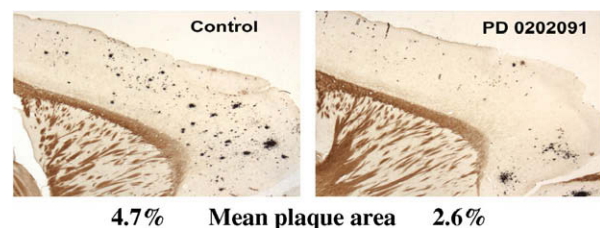
Compound	R ⁶	BASSR IC ₅₀ (μM)	BASST IC ₅₀ (μM)
48	4-NEt ₂	3	1
49	4-OMe	30	17
50	H	14	5
51	4-Me	9	1
52	3,4-Me	6	3
53	3-Br	2	3
54	2-Cl	6	2
55	3-Cl	4	3
56	4-Cl	3	2
57	3,4-Cl	25	1
58	2,4-Cl	2	2
59	3,5-Cl	3	3
60	3,4-F	8	5
61	4-F, 3-CF ₃	5	3

the same boost in potency as observed in the ethyl-linked series (Table 2).

The *in vivo* and pharmacokinetic data of **14** and **57**, pre-clinical chemical leads from the ethyl- and propyl-linked series, respectively, provided convincing evidence that this series of compounds

Table 5
Other modifications of propyl-linked derivative

Entry	R ⁷	R ⁸	BASSR IC ₅₀ (μM)	BASST IC ₅₀ (μM)
62	3,4-Cl	4-F	86	1
63	3,4-Cl	4-NO ₂	>100	1
64	3,4-Cl	4-Me	>100	>100
65	3,4-Cl	2-aza	60	5
66	3,4-Me	4-NO ₂	14	6
67	3,4-Me	4-F	>100	1
68	3,4-Me	2-aza	14	9
69	3,4-Me	3-F	12	5.4
70	3,4-Me	4-Me	16	3
71	4-OMe	3-F	14	9
72	4-OMe	4-F	14	10

**Figure 2.** Plaque density of control versus PD 0118057-treated Tg2576 mice, 200 mg/kg/day.**Figure 3.** Plaque density of control versus PD 0202091-treated Tg2576 mice, 60 mg/kg/day.

could potentially generate clinical candidates for Alzheimer's disease therapy. Figures 2 and 3 illustrate the reduction of senile plaques (black spots in cortex) in treated Tg2576 mice with PD 0118057 (**14**) and PD 0202091 (**57**), respectively, compared to an untreated control mouse.

As further noted in Figure 4, **57** showed a significant reduction in plaque load over a 7-month and then a 3-month treatment period at a lower dose versus **14**. A 3-fold lower dose of **57** versus **14** gave the same reduction in plaque load in the Tg2576 mouse.⁷

Additional evidence of these types of inhibitors preventing the aggregation of the Aβ protein was provided by an atomic force microscopy (AFM) study.⁸ Results indicated that smaller, fragmented Aβ species were present after *in vitro* treatment of the Aβ protein with, for example, **14** (Fig. 5).

This AFM result correlated with the smaller size Aβ peptide species observed by analytical ultracentrifugation (fibrils > 200S, fibrils treated with **14** = 15S).⁹ These Aβ species, although multimeric, seem to be non-toxic based on results from cell culture studies and the lack of cell loss in the mice. In contrast to amyloid fibrils, the fragmented Aβ species were protease-sensitive and thus could be cleared from the brain.⁹ The size of these accumulated Aβ

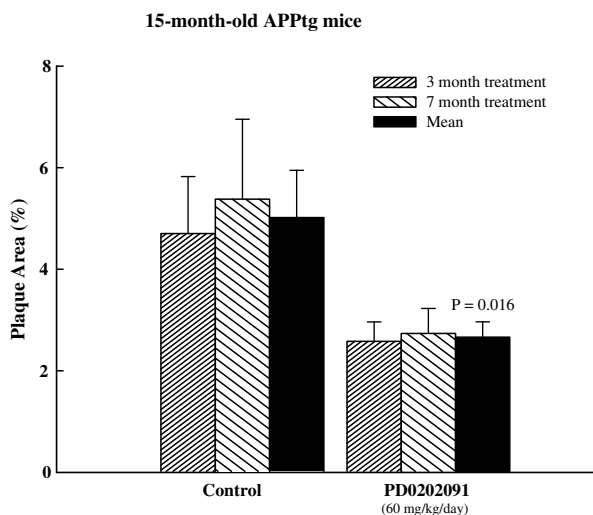


Figure 4. 3- and 7-month treatment of Tg2576 mice with PD 0202091.

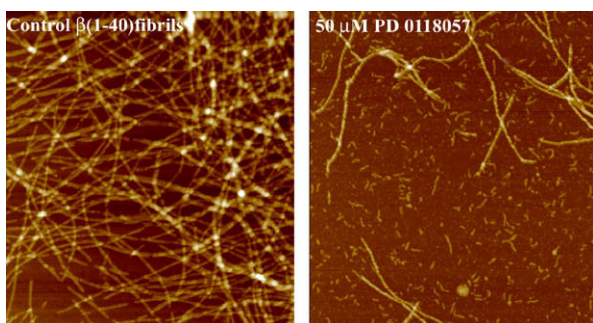


Figure 5. AFM results with PD 0118057 (14).

forms may indicate the inhibition site in the process of amyloid fibril formation, perhaps at an early, non-toxic pre-protofibril stage. Further study of the interruption of amyloid formation would be needed to establish the relationship of fibril deposition per se to the progression of Alzheimer's disease. Compounds such as **14** and **57** with brain penetration and significant in vivo activity could be useful in probing the role of fibril formation in disease progression.

Following the discovery of **14** and **57**, many amyloid aggregation inhibitors with low micromolar inhibition and in vivo efficacy were synthesized. However, **14** and **57** possessed the most acceptable drug-like properties, such as brain penetration, bioavailability, no toxicity and in vivo efficacy. Thus, the in vitro and in vivo effects of **14** and **57** indicate that in vitro inhibition of amyloid aggregation translated to efficacy in the Tg2576 mouse model as measured by the reduction in senile plaque load. These results suggest that agents limiting the self-polymerization of A β in brain and maintaining the A β in a metabolizable form can impede senile plaque formation, and hence, could lead to a disease-modifying drug for the treatment of Alzheimer's disease.

References and notes

- Selkoe, D. J.; Haass, C. *Nat. Rev. Mol. Cell Biol.* **2007**, *8*, 101.
- Augelli-Szafran, C. E.; Walker, L. C.; LeVine, H., III *Annu. Rep. Med. Chem.* **1999**, *34*, 21.
- Augelli-Szafran, C. E.; Bian, F.; Callahan, M. J.; Feng, R.; Iwai, A.; Lai, Y., LeVine, III, H.; Lipinski, W.; Walker, L. C.; Yasunaga, T. Abstracts of Papers, 228th National Meeting of the American Chemical Society, Philadelphia, PA; American Chemical Society: Washington, DC, 2004; Abstract MEDI-315.
- LeVine, H., III; Scholten, J. D. *Meth. Enzymol.* **1999**, *309*, 467.
- LeVine, H., III *Meth. Enzymol.* **1999**, *309*, 278.
- Callahan, M. J.; Lipinski, W. J.; Bian, F.; Durham, R. A.; Pack, A.; Walker, L. C. *Am. J. Pathol.* **2001**, *158*, 1173.
- Plaque reduction for **14** and **57** seems to be at maximum effect expected in this model: **14** (200 mg/kg/day, PO: 7 months ($n = 15$, 44% reduction)); **57** (60 mg/kg/day, PO: 7 months ($n = 14$, 47% reduction) and 3 months ($n = 16$, 45% reduction)).
- Thank you to P. Lansbury/J. Harper for AFM studies and J. Kelly/H. Lashuel for the analytical ultracentrifugation studies.
- Unpublished results.